Accelerating Super-Resolution Magnetic Resonance Imaging Using Toeplitz k-Space Matrices and Deep Learning Reconstruction

Krzysztof Malczewski[1] [0000−0002−6450−6444]

Institute of Information Technology
Warsaw University of Life Sciences
Warsaw, Poland
krzysztof_malczewski@sggw.edu.pl
https://wzim.sggw.edu.pl/?lang=en

Abstract. Magnetic Resonance Imaging (MRI) reconstruction remains a vital research domain, with ongoing efforts directed at enhancing image quality while minimizing acquisition time. Conventional k-space filling techniques have traditionally relied on Fourier transform properties and interpolation methods. However, recent innovations have introduced deep learning and compressed sensing as optimization strategies for this process. This study introduces a novel super-resolution framework that incorporates Toeplitz matrices for structured k-space completion, integrated with deep learning-based models and compressed sensing methodologies. Given their intrinsic connection to convolutional operations, Toeplitz matrices provide a mathematically sound foundation for defining k-space structures while ensuring data consistency.

Within this framework, deep neural networks are employed to infer the underlying k-space distribution in PROPELLER sequences from sparsely sampled data, while Toeplitz matrix constraints are utilized to maintain coherence. Additionally, the application of compressed sensing principles—incorporating sparsity priors and regularization techniques—improves both robustness and image quality, facilitating high-fidelity reconstructions from substantially undersampled acquisitions. The proposed approach is validated using both simulated and real MRI datasets, demonstrating that it effectively reduces reconstruction error and enhances image quality in comparison to traditional interpolation methods and standalone deep learning models. The findings indicate that combining sequentially rotating blade raw data acquisition with structured priors based on Toeplitz matrices, deep learning-driven inference, and compressed sensing optimization can yield more precise and computationally efficient MRI reconstructions, ultimately contributing to faster scan times in clinical applications.

Keywords: MRI · super-resolution · denoising · deep learning

1 Introduction

Over the past decade, Magnetic Resonance Imaging (MRI) has become an essential tool for diagnosing brain abnormalities. The need for high-resolution (HR) medical images is

ICCS Camera Ready Version 2025
To cite this paper please use the final published version:
DOI: 10.1007/978-3-031-97554-7_25

critical for detailed anatomical assessments, increasing the demand for improved visualization quality. However, hardware limitations in MRI scanners and constraints related to transmission bandwidth pose challenges in acquiring images at an optimal resolution for clinical use. Recent progress in image signal processing has introduced super-resolution reconstruction (SRR) techniques, which aim to overcome these constraints by enhancing MRI resolution.

Physical and hardware-related restrictions inherently limit the achievable resolution in MRI, often leading to prolonged scan durations, limited spatial coverage, and a reduced signal-to-noise ratio (SNR). Super-resolution (SR) remains a complex challenge, as it requires the reconstruction of high-resolution images from low-resolution data while preserving structural integrity and texture. Typically, this process is modeled as a convex optimization problem that necessitates effective regularization strategies to maintain consistency in the reconstructed images. Traditional regularization methods, such as total variation (TV) constraints, operate under the assumption of piecewise smoothness, which can sometimes fail to retain intricate local details. Deep learning-based SR techniques address these issues by learning complex mappings between low-resolution and high-resolution images, leading to improved reconstruction quality.

Recent studies have demonstrated that deep convolutional neural networks (CNNs) are highly effective in SRR tasks [32], particularly in Single Image Super-Resolution (SISR) [2]. CNN-based approaches, such as Super-Resolution CNNs (SRCNNs) and their more advanced counterparts, have successfully generated high-quality SR images in natural image processing. Earlier SR techniques relied on patch-based, edge-based [4], sparse coding, and statistical models [3] , which, despite being computationally efficient, exhibited limitations in recovering detailed structural information. The introduction of CNNs has significantly advanced SR performance, making them a preferred choice for medical imaging applications [10].

Nevertheless, initial deep learning models encountered difficulties in super-resolving 3D medical images, as they processed slices individually and failed to consider three-dimensional spatial dependencies. While 3D models offer better spatial consistency [29], they come with high computational costs and memory demands. Conventional evaluation metrics, such as Mean Squared Error (MSE) and Peak Signal-to-Noise Ratio (PSNR) [7], are often used to assess image quality but may not fully capture perceptual accuracy, sometimes resulting in reconstructions with diminished sharpness. Multi-Level Densely Connected Super-Resolution Networks (mDCSRN) [7] have been introduced to address these shortcomings by leveraging densely connected architectures and Wasserstein Generative Adversarial Networks (WGANs) to refine SR reconstructions [9]. These networks effectively enhance intensity differences while maintaining computational efficiency.

Generative Adversarial Networks (GANs) have gained widespread attention in SR applications due to their ability to restore fine details and high-frequency image components. However, challenges such as noise amplification and image distortions persist, necessitating improvements in optimization strategies. In medical imaging, GAN-based models have been incorporated alongside compressed sensing (CS) to improve MRI reconstruction. Hybrid frameworks combining CNNs with k-space correction have demon-

ICCS Camera Ready Version 2025
To cite this paper please use the final published version:
DOI: 10.1007/978-3-031-97554-7_25

strated promising results in restoring missing information and reducing aliasing artifacts, as exemplified in architectures like KIKI-Net [10].

Parallel imaging and sparse sampling methods have played a significant role in accelerating MRI data acquisition. Parallel imaging techniques, including Sensitivity Encoding (SENSE) and Generalized Autocalibrating Partially Parallel Acquisitions (GRAPPA), rely on multi-coil signals to reconstruct undersampled k-space data [11]. Conversely, sparse sampling techniques utilize prior information, such as sparsity priors and low-rank constraints, to recover missing data. Recent advancements have capitalized on structured matrix representations (e.g., Toeplitz and Hankel matrices) to exploit linear dependencies in k-space, resulting in improved image reconstructions [12].

Despite the success of deep learning in MRI reconstruction, one of its major limitations is the tendency of CNN-based approaches to oversmooth high-frequency details. Traditional loss functions, such as MSE and Structural Similarity Index Measure (SSIM), do not always align with perceptual accuracy, leading to suboptimal reconstructions. To address this, recent studies have explored feature-based loss functions and perceptual metrics, particularly in GAN-based models [9]. However, training GANs remains challenging due to instability issues and the potential hallucination of nonexistent structures.

This research introduces a novel MRI reconstruction approach that integrates deep learning, compressed sensing, and structured k-space priors to enhance resolution while minimizing acquisition times. The proposed framework incorporates Toeplitz matrices [13] for structured k-space filling in PROPELLER sequences and employs SPIRiT (Iterative Self-Consistent Parallel Imaging Reconstruction) to improve reconstruction accuracy. By enforcing bidirectional low-rank constraints, the model ensures k-space consistency while reducing computational overhead. Additionally, the use of Wasserstein GANs (WGANs) helps preserve texture fidelity, leading to perceptually improved super-resolution images.

The effectiveness of this method is validated through extensive experiments on both simulated and real MRI datasets. The results demonstrate that the proposed approach significantly enhances reconstruction quality by preserving texture and suppressing artifacts more effectively than conventional CNN-based and interpolation-based techniques. These findings suggest that combining structured k-space priors, compressed sensing, and deep learning inference can lead to more efficient and accurate MRI reconstructions, thereby enabling faster and higher-quality clinical imaging.

2 Challenges in K-Space Filling Acceleration and the Proposed Solution

SPIRiT (Iterative Self-Consistent Parallel Imaging Reconstruction) is an advanced technique developed to improve parallel MRI reconstruction by maintaining self-consistency across multi-coil k-space data [14]. As depicted in Figure 4, the procedure begins with the estimation of linear dependencies between intra- and inter-coil k-space data within a localized region of the fully sampled central k-space, known as the Auto-Calibration Signal (ACS) [15]. These estimated dependencies are then extended throughout the remaining k-space data to ensure consistency in calibration. Mathematically, this relationship can be represented as:

ICCS Camera Ready Version 2025
To cite this paper please use the final published version:
DOI: 10.1007/978-3-031-97554-7_25

$$X = \mathcal{G}X \tag{1}$$

where X represents the k-space data collected from all coils, and $\mathcal{G}$ serves as an operator that applies convolution to the k-space data using calibration kernels derived from the ACS region. The data acquisition process follows the equation:

$$Y = \mathcal{U}X \tag{2}$$

where Y signifies the sampled k-space data, with non-acquired positions zero-filled, while $\mathcal{U}$ denotes the undersampling operator. The SPIRiT reconstruction is then formulated as an optimization problem:

$$\min_X |\mathcal{G}X - X|_F^2 \qquad |Y_s - UX_s|_F^2 \leq \epsilon \tag{3}$$

where $|\cdot|_F$ denotes the Frobenius norm, and ϵ represents an upper bound on measurement noise. Research findings indicate that SPIRiT outperforms conventional parallel imaging techniques such as SENSE and GRAPPA [16], yielding improved image quality [**?**].

To further enhance image regularization, an additional constraint is introduced in the SPIRiT objective function, leading to the development of the L1-SPIRiT model [17]:

$$\min_X |\mathcal{G}X - X|_F^2 + \lambda |\Psi F^{-1} X|_1 \qquad |Y_s - UX_s|_F^2 \leq \epsilon \tag{4}$$

where Ψ represents the sparse transform, F^{-1} corresponds to the inverse Fourier transform, and λ serves as a weighting factor to balance the trade-off between sparsity enforcement and calibration consistency.

Proposed Approach: Low-Rank Constraints in PROPELLER Blades

In this study, a novel strategy is introduced that applies simultaneous low-rank constraints on k-space along both horizontal and vertical orientations:

$$T_{PROPELLER} \min_{X_s} \|\mathcal{T}W^{\perp} X_s^*\| + \|\mathcal{T}W X_s^*\| + \beta_2 \|Y_s - UX_s\|_F^2 \tag{5}$$

where W and $W^{\perp}$ denote Fourier transform weightings corresponding to horizontal and vertical filters, respectively. The nuclear norm $\|\cdot\|^*$ enforces a low-rank constraint on the weighted Toeplitz-structured matrix. This method diverges to some extent from existing approaches [18] by independently applying weighting constraints, thereby lowering computational complexity, see Figure 1.

Learning Priors in Toeplitz-Structured k-Space

Deep learning models typically rely on large datasets for effective training. Instead, this work leverages **Toeplitz matrices** to synthetically generate training samples. The training process consists of three key steps:

ICCS Camera Ready Version 2025
To cite this paper please use the final published version:
DOI: 10.1007/978-3-031-97554-7_25

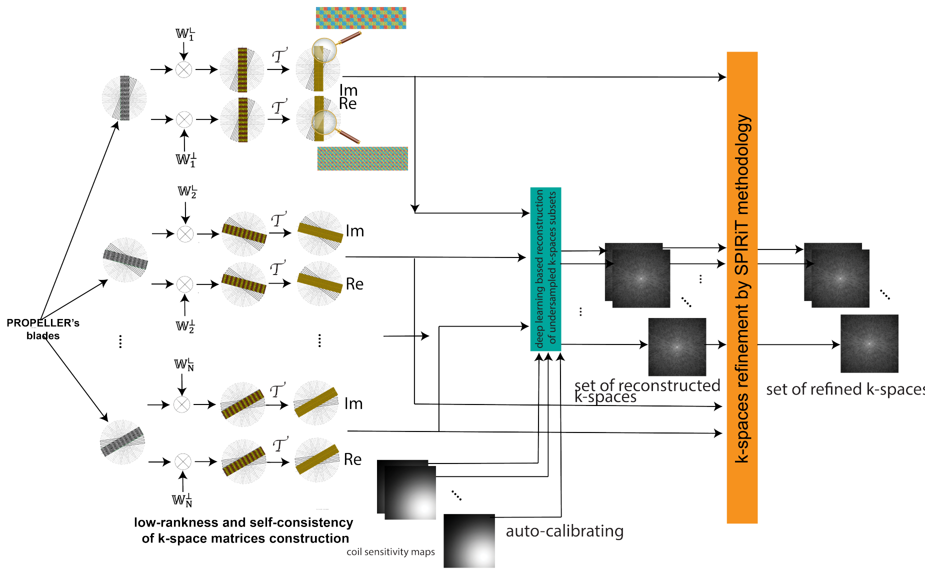

Fig. 1: Toeplitz matrices of PROPELLER blades generating

Step 1: Constructing a Large Toeplitz Matrix A sliding window of dimensions (8x8x8) is applied across PROPELLER's blade to construct an extensive block Toeplitz matrix, see Figure 2:

$$\mathcal{T}_k = t(k) \tag{6}$$

Step 2: Isolating PROPELLER's Blades's Patches Following prior studies [**?**], multiple Toeplitz-structured k-space patches $\{P_{k_i}^j\}_{j=1}^N$ of size 256x256 are extracted, producing 484 patch samples,. Singular value decomposition analysis verifies that these patches retain low-rank properties.

Step 3: Modeling Internal k-Space Statistics The redundancy in overlapping patches is utilized to learn statistical distributions. A **score-based network** is employed to capture the internal structure via a diffusion process:

$$dP_k = f(P_k, t)dt + g(P_k)dw \tag{7}$$

Following the **Variance Exploding (VE) Stochastic Differential Equation (SDE) framework** [19], the model is formulated as:

$$P_k^j = P_k^{j-1} + \sqrt{\sigma_j^2 - \sigma_{j-1}^2} z_{j-1}, \quad j = 1, L, N \tag{8}$$

ICCS Camera Ready Version 2025
To cite this paper please use the final published version:
DOI: 10.1007/978-3-031-97554-7_25

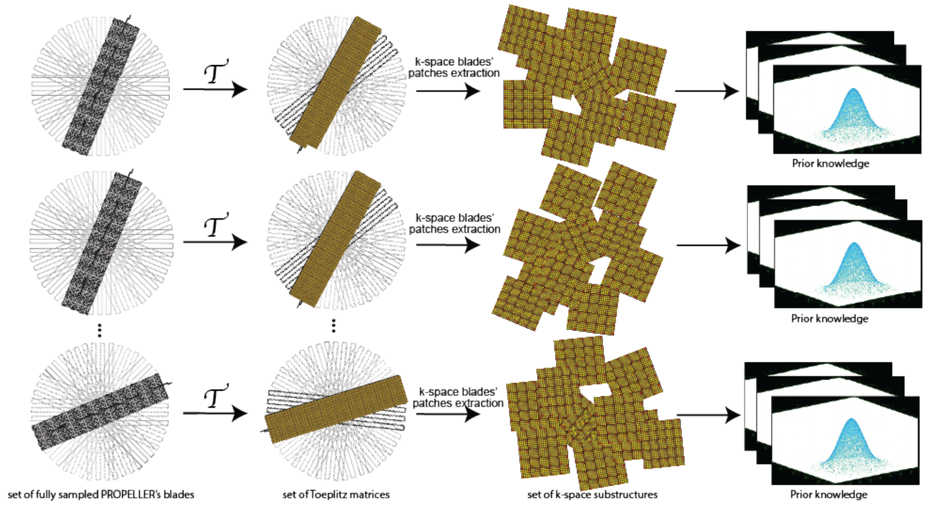

Fig. 2: Toeplitz matrices generation

where $\sigma(t)$ denotes a Gaussian noise function. The final optimization objective is given by:

$$\theta^* = \arg\min_{\theta} \alpha_t E_{R_k}[S_\theta(R_k, t) - \nabla_{R_k} \log p_t(R_k|R_0)]^2 \tag{9}$$

This methodology significantly enhances MRI reconstruction while minimizing computational burden.

Enhancement of k-Space Using SPIRiT

The refinement process necessitates three input components: the undersampled k-space data, the SPIRiT kernel derived from the ACS region of the undersampled k-space, and the deep learning (DL) reconstructed k-space. Figure 4 provides a comprehensive illustration of the proposed refinement framework.

Deriving the SPIRiT Kernel

The first stage involves estimating the SPIRiT kernel, a process termed auto-calibration. Prior to calibration, the **Virtual Conjugate Coil (VCC)** technique [20] is utilized to effectively double the number of imaging channels. This approach improves the conditioning of the SPIRiT reconstruction problem. The calibration region is then transformed into a calibration matrix by sweeping the kernel across it and constructing a block-Hankel structure [12]. Singular value thresholding is subsequently applied to the calibration matrix using a predefined threshold, followed by the estimation of the SPIRiT kernel through Tikhonov-regularized least squares, yielding an analytical solution [14].

ICCS Camera Ready Version 2025
To cite this paper please use the final published version:
DOI: 10.1007/978-3-031-97554-7_25

Optimization Framework

The refinement process is formulated as the following constrained optimization problem:

$$\arg\min_{k} \|Dk - y\|^2 + \lambda_1 \|(G - I)k\|^2 + \lambda_2 \|D_c(k - \tilde{k})\|^2, \quad (10)$$

where D_c is the operator that selects unacquired k-space positions, and $\tilde{k}$ represents the DL-reconstructed k-space.

To solve this problem, the **conjugate gradient (CG) algorithm** is employed with 250 iterations per one PROPELLER's blade. Additional implementation details are presented in the following manner: **Input:** Acquired k-space blade (y) and DL-reconstructed k-space ($\tilde{k}$). **Output:** Refined fully dimensional k-space. **Procedure:** 1. Apply Virtual Conjugate Coil (VCC) augmentation to y and $\tilde{k}$. 2. Compute the SPIRiT kernel using y. 3. Estimate transformation matrix $(G - I)$ from ACS lines. 4. Solve optimization using conjugate gradient minimization.

3 Reconstruction of MR Images from Set of Refined k-spaces via Convolutional Neural Networks

Several advanced Convolutional Neural Network (CNN) architectures have been proposed for image reconstruction tasks. The method presented in this study employs a fully convolutional network, which has been well-documented in prior research [21]. This choice is based on its strong performance in medical imaging applications.

The encoding process follows a traditional CNN approach, utilizing sequential two-dimensional 3×3 convolutional layers. Each layer undergoes batch normalization, activation using a leaky rectified linear unit (Leaky ReLU), and downsampling through a 2×2 max-pooling operation.

Fig. 3: Low-resolution k-space MR image reconstruction and registration layer

The primary objective of this study is to reconstruct high-quality magnetic resonance images from sparsely sampled k-space data. A conjugate symmetry-based mask is used to optimize the sampling process, reducing acquisition time while preserving

ICCS Camera Ready Version 2025
To cite this paper please use the final published version:
DOI: 10.1007/978-3-031-97554-7_25

essential structural information. Image enhancement procedures, including deblurring and registration layers, mitigate motion artifacts and blurring effects.

The proposed U-Net model [22] was trained using the mean squared error (MSE) loss function, formulated as follows:

$$\beta^i = \begin{cases} \underset{\beta^i}{\arg\min} \left\| \chi_{true} - f_{\beta^i}\left(|F^{-1}(y_0)|\right) \right\| & i = 0 \\ \underset{\beta^i}{\arg\min} \left\| \chi_{true} - f_{\beta^i} - f_{\beta^i}(\chi^i) \right\| & \text{otherwise} \end{cases} \tag{11}$$

The Adam optimizer [23] was utilized with a learning rate of 0.0001 for 100 training epochs, using a dataset comprising 32 images. Hyperparameters were determined empirically based on prior experimentation.

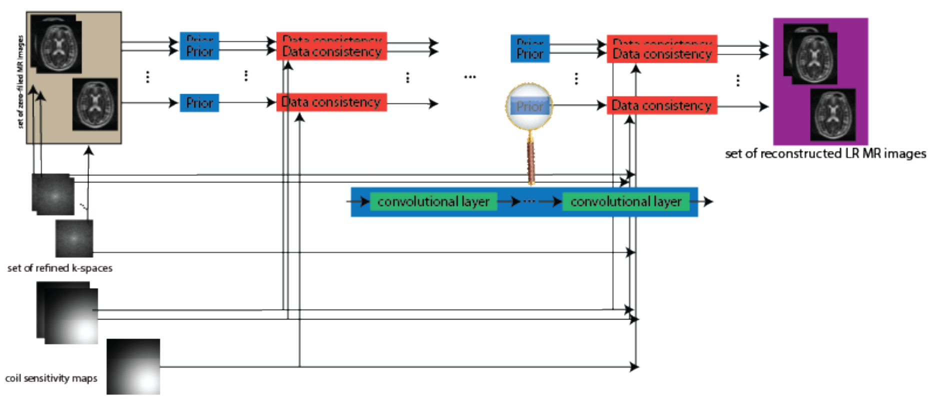

Fig. 4: Set of Low Resolution MR images reconstruction from set of refined k-spaces

4 Super-Resolution Image Reconstruction via Generative Adversarial Networks (GANs)

A GAN-based framework incorporating deformable motion estimation and reconstruction networks is utilized. The model consists of generator and discriminator blocks, optimizing image restoration while correcting missing details.

$$\min_{\mathcal{G}} \max_{\mathcal{D}} \mathbb{E}_x \left[\log \left(\mathcal{D}(x) \right) \right] - \mathbb{E}_y \left[\log \left(1 - G(y) \right) \right] \tag{12}$$

where y and x represent degraded and restored images, respectively.

The generator network employs a residual block structure to improve efficiency and reduce parameter count. Discriminator architecture comprises eight convolutional layers, where feature resolution progressively reduces to maintain representational consistency.

ICCS Camera Ready Version 2025
To cite this paper please use the final published version:
DOI: 10.1007/978-3-031-97554-7_25

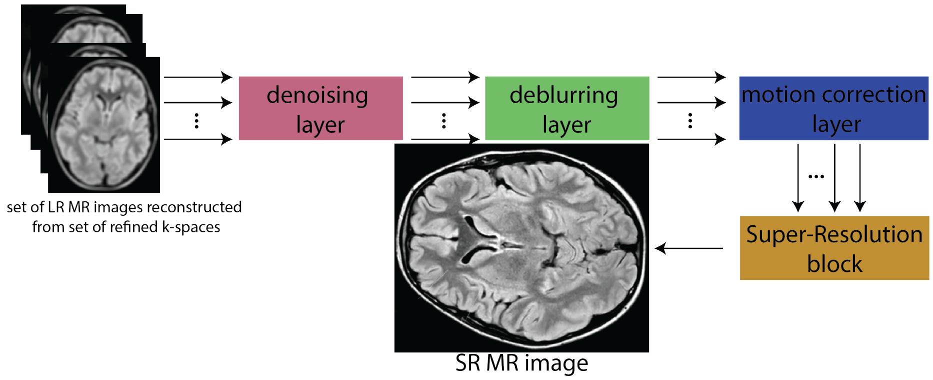

Fig. 5: Main SR algorithm's flowchart

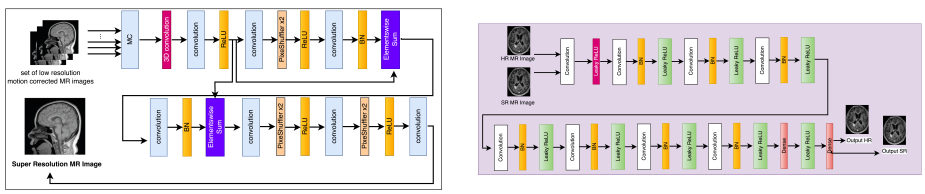

Fig. 6: Generator and Discriminator network architectures. (a) Structure of the generator network. (b) Discriminator network architecture.

5 High-Resolution MRI Reconstruction Techniques

Image reconstruction begins with undersampled k-space data, applying noise reduction, deblurring, and motion estimation techniques [24]. The Wasserstein GAN (WGAN) enhances adversarial network stability, utilizing the Earth Mover's distance:

$$\mathcal{W}(\mathcal{P}_{ref}, \mathcal{P}_{gen}) = \frac{1}{K} \sup_{||f||_{L \leq K}} \mathbb{E}_{(x,y)\sim\mathcal{P}_{ref}}[f(x)] - \mathbb{E}_{x\sim\mathcal{P}_{gen}}[f(x)] \tag{13}$$

This metric improves gradient calculations, mitigating instability during training. Loss functions are defined as:

$$D_{loss} = \mathbb{E}_{x\sim\mathcal{P}_{gen}}[f_{\mathcal{W}}(x)] - \mathbb{E}_{x\sim\mathcal{P}_{ref}}[f_{\mathcal{W}}(x)] \tag{14}$$

$$G_{loss} = \mathbb{E}_{x\sim\mathcal{P}_{gen}}[f_{\mathcal{W}}(x)] \tag{15}$$

Ensuring sharper reconstructions, a hybrid perceptual loss function combining MSE and feature loss is employed:

$$\mathcal{L}_{perceptual} = \frac{1}{abc}||\varpi(G(x)) - \varpi(y)||_F^2 \tag{16}$$

ICCS Camera Ready Version 2025
To cite this paper please use the final published version:
DOI: 10.1007/978-3-031-97554-7_25

where ϖ denotes a feature extraction function, leveraging the pre-trained VGG-19 network [25].

6 Results

The effectiveness of the proposed methodology was assessed through both controlled laboratory experiments and in-vivo evaluations. The primary goal of this research was to analyze and compare various super-resolution techniques and k-space sampling strategies. The performance of a novel approach for generating high-resolution images was investigated by benchmarking it against several state-of-the-art methodologies. Additional experiments were conducted to examine how different k-space decimation ratios impact the quality of reconstructed magnetic resonance (MR) images.

A detailed comparative study was performed to explore the effects of different k-space sampling patterns on magnetic resonance imaging (MRI). The corresponding results are illustrated in Figure 7. The findings suggest that incorporating compressed sensing methodologies, alongside the principles of Hermitian symmetry and partial Fourier reconstruction, can significantly reduce the time required for k-space acquisition when compared to conventional sampling methods. The supporting statistical evidence is presented in Table 1, highlighting the importance of this observation.

The experimental setup involved compressing raw MRI signals by employing sampling rates corresponding to 20-40-60-80-100% of the fully sampled k-space data. The core objective of this research is to integrate super-resolution image reconstruction with sparse sampling strategies within the MRI scanner's k-space. The compression of PROPELLER blades was executed precisely by reducing radial trajectories to 30 and 15 paths in the frequency domain. This study sought to develop a sparsity-driven model aimed at enhancing image reconstruction from projections acquired at smaller angles. Specifically, image reconstructions were based on a reduced set of fifty projections constrained within a $\pi/2$ aperture. Additionally, nonrigid and deformable transformations were introduced to simulate distortions in the original magnetic resonance images.

For accurate replication of MRI images, a range of preprocessing techniques was applied to the collected data, including Gaussian blurring, noise addition, and downsampling. Since publicly available datasets containing motion-distorted images were not accessible, artificially generated data were utilized to evaluate the proposed methodology. The images analyzed in this study were sourced from the anonymized database of the Medical University in Poznań and the Multimodal Brain Tumor Image Segmentation Benchmark dataset (reference [26]). Motion artifacts were artificially introduced into static images following the approach outlined in [27]. These motion-corrupted datasets were subsequently used to assess the performance of motion correction algorithms, as described in [28].

The methodology involved simulating motion effects within motion-free k-space data for each PROPELLER blade, followed by segmenting specific portions of the k-space data. These segments were then recombined to generate the required sample patterns. The dataset was integral to the domain of image processing. The creation of simulated k-space multishot MRI data was successfully executed using the techniques outlined in[28].

ICCS Camera Ready Version 2025
To cite this paper please use the final published version:
DOI: 10.1007/978-3-031-97554-7_25

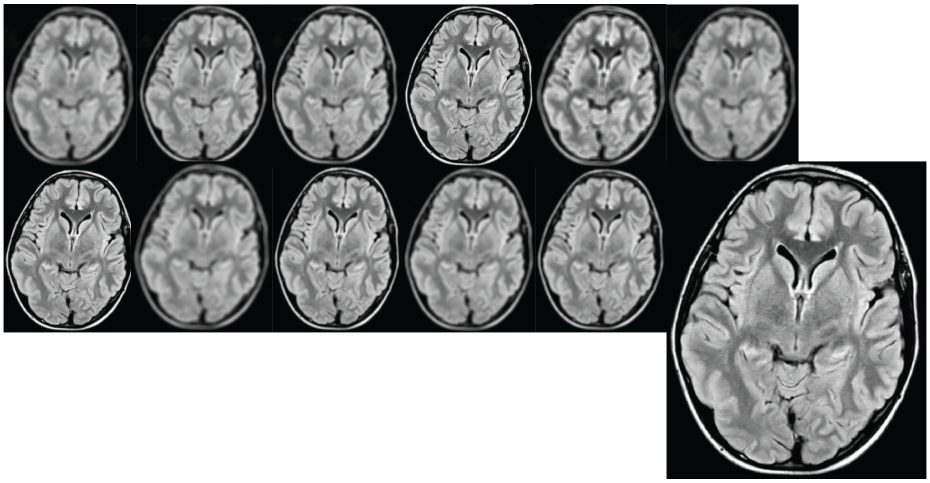

Fig. 7: Clinical trial analysis depicting various reconstruction methods. The first row illustrates reconstructions without motion correction or super-resolution reconstruction (SRR). The second row presents various reconstruction methodologies, including B-spline interpolation (2), Yang's approach [29] (3), Lim's method [38] (4), Zhang's technique [31] (5), Kim's algorithm [32] (6), Mahapatra's approach [33] (7), Liu et al.'s method [34] (8), Dong's technique [35] (9), Pham et al.'s approach [36] (10), Shi's method [37] (11), and the author's proposed technique [38] (12). Motion correction and sampling strategies were employed to achieve super-resolution, with a compression ratio of 50%.

Table 1: Comparison of scanning parameters utilized for Figure 7.

Sampling Scheme	TR	TE	FOV	Voxel Size (mm)	Acquisition Time (s)	p-value
PROPELLER 3.0	1223	186	290	0.96/0.96/1.00	367	0.149
SENSE-ASSET	1220	188	290	0.96/0.96/1.00	366	0.215
GRAPPA-ARC	1245	188	290	0.96/0.96/1.00	416	0.129
VarNet and Refined k-space	1258	190	280	0.96/0.96/1.00	142	0.126
Refined PROPELLER	1218	183	280	0.96/0.93/1.00	105	0.103

Results and final remarks Medical imaging often faces challenges such as low spatial resolution, contrast limitations, visual noise, and blurring, which can impact diagnostic accuracy.

This study introduces a novel MRI reconstruction method combining the Wasserstein Generative Adversarial Network (WGAN) with deformable motion registration to enhance image quality, particularly in compressed sensing (CS) MRI sequences. The model leverages sequential MR data, ensuring stable training and outperforming existing methods in Peak Signal-to-Noise Ratio (PSNR), Mean Absolute Error (MAE), and

ICCS Camera Ready Version 2025
To cite this paper please use the final published version:
DOI: 10.1007/978-3-031-97554-7_25

Table 2: Evaluation of the proposed algorithm at varying k-space compression ratios (Figure 7).

Residual k-space Samples (%)	PSNR (dB)	MAE	IEM
10	14.92	24.40	1.23
20	19.19	20.58	1.85
30	20.57	19.72	1.85
40	26.61	18.11	1.95
50	26.64	18.10	2.45
60	29.59	17.19	3.76
70	30.20	16.83	3.78
80	29.65	16.24	4.01
90	31.42	15.79	4.02
100	33.57	13.39	4.54

Table 3: Combined data for PSNR, MAE, and IEM metrics.

SRR procedure	N	PSNR		MAE		IEM	
		M	SD	M	SD	M	SD
SR-no, MC-no	100	22.305	0.01	21.906	0.01	21.815	0.01
SR-no, MC-yes	100	25.204	0.01	25.085	0.01	24.896	0.01
cubic spline, MC-yes	100	23.724	0.01	23.954	0.01	24.277	0.01
Yang's	100	26.817	0.01	27.146	0.01	27.667	0.01
Lim's	100	30.434	0.01	30.475	0.01	29.738	0.01
Zhang's	100	30.12	0.01	29.28	0.01	29.698	0.01
Zhang's no. 2	100	30.876	0.02	30.893	0.021	30.486	0.02
Mahapatra et al.	100	29.832	0.01	29.482	0.01	29.775	0.01
Liu et al.	100	29.151	0.042	28.616	0.041	28.476	0.041
Dong et al.	100	27.293	0.01	27.029	0.01	26.665	0.01
Pham et al.	100	24.222	0.042	24.57	0.042	24.617	0.041
Shi et al.	100	30.5	0.031	31.356	0.031	30.327	0.031
The proposed algorithm	100	33.228	0.01	33.828	0.01	32.918	0.01

Image Enhancement Measure (IEM). It significantly improves texture restoration and high-frequency detail reconstruction.

The proposed approach integrates iterative optimization in image and k-space domains, reducing aliasing artifacts and enhancing image clarity. Evaluation on public datasets confirmed superior performance in preserving fine details. The method improves PSNR across different sampling rates and effectively processes real-valued MR images. Future research will explore clinical applications, focusing on T1-weighted imaging.

This technique enhances image quality while reducing acquisition times, mitigating artifacts from sparse data. It integrates compressed sensing, raw data sparsity optimization, and super-resolution reconstruction, efficiently filling k-space and refining

ICCS Camera Ready Version 2025
To cite this paper please use the final published version:
DOI: 10.1007/978-3-031-97554-7_25

edge representation. The method is compatible with MRI scanners without hardware modifications.

Experimental results, illustrated in Figure 7, confirm improved resolution and diagnostic clarity. The approach enhances the detection of malignant anomalies, validated through PSNR assessments.

Comparative analysis against state-of-the-art super-resolution methods demonstrates significant improvements, evaluated using statistical tests. Results indicate a robust enhancement in PSNR, confirming the method's effectiveness.

This study presents a GAN-based MRI reconstruction framework incorporating denoising and deformable motion estimation. It effectively reduces noise and artifacts, outperforming conventional methods in cardiac MR imaging and aiding in precise diagnoses.

The proposed refinement technique, assessed through k-space and image comparisons, corrects errors in deep learning-based reconstructions, enhancing texture and preserving fine details. Statistical analysis of image quality metrics (PSNR, SSIM, HFEN, and GMSD) confirms improved high-frequency image retention.

This study introduces a SPIRiT-based refinement framework that enhances deep learning reconstructions by enforcing k-space consistency, restoring intricate structures like microvascular networks. Future research will explore additional constraints to further optimize performance.

Potential clinical benefits include improved visualization of ligaments and small-scale structures, with further validation involving lesion assessments by radiologists. Future work will focus on acceleration through algorithmic optimizations, parallelization, and comparisons with unrolled neural networks and GAN-based methods.

References

1. Jiwon Kim, Jung Kwon Lee, and Kyoung Mu Lee. Deeply recursive convolutional network for image super-resolution. In 2016 IEEE CVPR 2016, Las Vegas, NV, USA, June 27-30, 2016, pages 1637–1645, 2016. Resonance in Medicine, 2009, 62, (3), pp. 706-716
2. Bee Lim, Sanghyun Son, Heewon Kim, Seungjun Nah, and Kyoung Mu Lee, Enhanced deep residual networks for single image super-resolution, In 2017 IEEE Conference on Computer Vision and Pattern Recognition Workshops, CVPR Workshops 2017, Honolulu, HI, USA, July 21-26, 2017, pages 1132–1140, 2017.
3. Lidke, K.A.; Rieger, B.; Jovin, T.M.; Heintzmann, R., Superresolution by localization of quantum dots using blinking statistics, Opt. Express 2005, 13, 7052–7062.
4. Tai, Y.W.; Liu, S.; Brown, M.S.; Lin, S. Super resolution using edge prior and single image detail synthesis. In Proceedings of the IEEE CSCCVPR, San Francisco, CA, USA, 13–18 June 2010.
5. Eo, T.; Jun, Y.; Kim, T.; Jang, J.; Lee, H.J.; Hwang, D., KIKI-net: Cross-domain convolutional neural networks for reconstructing undersampled magnetic resonance images, Magn. Reson. Med. 2018, 80, 2188–2201.
6. Yang F., Ding M. and Zhang X., Non-Rigid Multi-Modal 3D Medical Image Registration Based on Foveated Modality Independent Neighborhood Descriptor, Sensors Journal, 19(21), 4675, 2019.
7. K. Malczewski, Super-Resolution with compressively sensed MR/PET signals at its input, Informatics in Medicine Unlocked, Volume 18, 2020.

ICCS Camera Ready Version 2025
To cite this paper please use the final published version:
DOI: 10.1007/978-3-031-97554-7_25

8. Huang, G.; Liu, Z.; van der Maaten, L.; Weinberger, K.Q., Densely Connected Convolutional Networks, In Proceedings of the 2017 IEEE CSCCVPR, Honolulu, HI, USA, 21–26 July 2017; pp. 4700–4708.
9. Arjovsky, M., Chintala, S., and Bottou, L., Wasserstein GAN, ICML, 2017.
10. Eo, T.; Jun, Y.; Kim, T.; Jang, J.; Lee, H.J.; Hwang, D., KIKI-net: Cross-domain convolutional neural networks for reconstructing undersampled magnetic resonance images, Magn. Reson. Med. 2018, 80, 2188–2201.
11. Ding Y, Chung YC, Jekic M, Simonetti OP, A new approach to auto-calibrated dynamic parallel imaging based on the Karhunen-Loeve transform: KL-TSENSE and KL-TGRAPPA, Magn Reson Imaging. 2011;65:1786–1792.
12. Hu, Y., Peng, Y., Wang, Y., Wang, S., Qu, X.: One-shot Generative Prior in Hankel-k-space for Parallel Imaging Reconstruction. IEEE Trans. Med. Imaging (2023).
13. Malczewski, K., Stasinski, R.: Toeplitz-based iterative image fusion scheme for MRI. In: 15th IEEE International Conference on Image Processing (ICIP), pp. 833–836. IEEE (2008).
14. Lustig, M., Pauly, J.M.: SPIRiT: Iterative self-consistent parallel imaging reconstruction from arbitrary k-space. Magn. Reson. Med. **64**, 457–471 (2010).
15. Chang, Y., Pham, H.A., Li, Z.: A dual-interpolator method for improving parallel MRI reconstruction. Magn. Reson. Imaging 92, 108–119 (2022).
16. Ding Y, Chung YC, Jekic M, Simonetti OP, A new approach to auto-calibrated dynamic parallel imaging based on the Karhunen-Loeve transform: KL-TSENSE and KL-TGRAPPA, Magn Reson Imaging. 2011;65:1786–1792.
17. Murphy, M., Alley, M., Demmel, J., Keutzer, K., Vasanawala, S., Lustig, M.: Fast l1-SPIRiT compressed sensing parallel imaging MRI: scalable parallel implementation and clinically feasible runtime. IEEE Trans. Med. Imaging. 31(6), 1250–1263 (2012).
18. Pan, T., Duan, J., Wang, J., Liu, Y.: Iterative self-consistent parallel magnetic resonance imaging reconstruction based on nonlocal low-rank regularization. arXiv preprint arXiv:2108.04517 (2021).
19. Song, Y., Sohl-Dickstein, J., Kingma, D.P., Kumar, A., Ermon, S., Poole, B.: Score-Based Generative Modeling through Stochastic Differential Equations. In: International Conference on Learning Representations (ICLR) (2021).
20. Blaimer, M., Gutberlet, M., Kellman, P., Breuer, F.A., Köstler, H., Griswold, M.A.: Virtual coil concept for improved parallel MRI employing conjugate symmetric signals. Magn. Reson. Med. 61(1), 93–102 (2009).
21. Du, J., Sun, J., Zhang, W., Xu, Z., Tao, D.: Fully convolutional measurement network for compressive sensing image reconstruction. arXiv preprint arXiv:1712.01641 (2017).
22. Ronneberger, O., Fischer, P., Brox, T.: U-Net: Convolutional Networks for Biomedical Image Segmentation. In: Navab, N., Hornegger, J., Wells, W., Frangi, A. (eds.) MICCAI 2015. LNCS, vol. 9351, pp. 234–241. Springer, Cham (2015).
23. Kingma, D.P., Ba, J.: Adam: A Method for Stochastic Optimization. In: International Conference on Learning Representations (ICLR) (2015).
24. Hu, X.; Mu, H.; Zhang, X.; Wang, Z.; Tan, T.; Sun, J., Meta-SR: A Magnification-Arbitrary Network for Super-Resolution, In Proceedings of the 2019 IEEE/CVF Conference on Computer Vision and Pattern Recognition (CVPR), Long Beach, CA, USA, 16–20 June 2019; pp. 1575–1584.
25. Simonyan, K., Zisserman, A., Very deep convolutional networks for large-scale image recognition. Computer Science, 2014.
26. Menze, B.H., et al.: The Multimodal Brain Tumor Image Segmentation Benchmark (BRATS). IEEE Trans. Med. Imaging 34(10), 1993–2024 (2015).
27. Brosch, T., Zaitsev, M., Spoormaker, V.I., Polimeni, J.R., Weiskopf, N.: Reproduction of motion artifacts for performance analysis of prospective motion correction in MRI. Magn. Reson. Med. 71(1), 182–190 (2014).

ICCS Camera Ready Version 2025
To cite this paper please use the final published version:
DOI: 10.1007/978-3-031-97554-7_25

28. Malczewski, K.: A Framework for Reconstructing Super-Resolution Magnetic Resonance Images from Sparse Raw Data Using Multilevel Generative Methods. Appl. Sci. 14(4), 1351 (2024).
29. Yang F., Ding M. and Zhang X., Non-Rigid Multi-Modal 3D Medical Image Registration Based on Foveated Modality Independent Neighborhood Descriptor, Sensors Journal, 19(21), 4675, 2019.
30. Lim, B.; Son, S.; Kim, H.; Nah, S.; Lee, K.M., Enhanced Deep Residual Networks for Single Image Super-Resolution, In Proceedings of the 2017 IEEE CVPRW, Honolulu, HI, USA, 21–26 July 2017; pp. 1132–1140.
31. Yulun Zhang, Yapeng Tian, Yu Kong, Bineng Zhong, and Yun Fu, Residual dense network for image super-resolution, In 2018 IEEE Conference on Computer Vision and Pattern Recognition, CVPR 2018, Salt Lake City, UT, USA, June 18-22, 2018, pages 2472–2481, 2018.
32. Jiwon Kim, Jung Kwon Lee, and Kyoung Mu Lee. Deeply recursive convolutional network for image super-resolution. In 2016 IEEE Conference on Computer Vision and Pattern Recognition, CVPR 2016, Las Vegas, NV, USA, June 27-30, 2016, pages 1637–1645, 2016. Resonance in Medicine, 2009, 62, (3), pp. 706-716
33. Mahapatra, D., Bozorgtabar, B. & Garnavi, R. Image super-resolution using progressive generative adversarial networks for medical image analysis. Comput. Med. Imaging Graph. 71, 30-39, 2019.
34. C. Liu, et al., Fusing multi-scale information in convolution network for MR image super-resolution reconstruction., Biomedical engineering online, 2018, pp.114.
35. Dong C., et al., Learning a deep convolutional network for image super-resolution, In: European Conference on Computer Vision, pp. 184–199, 2014.
36. Pham et al.'s [36] CH, Tor-Díez C, Meunier H, Bednarek N, Fablet R, Passat N, et al., Multiscale brain MRI super-resolution using deep 3D convolutional networks, Comput Med Imaging Graph., 2019.
37. Shi, W.; Jiang, F.; Zhang, S.; Zhao, D., Deep networks for compressed image sensing, In Proceedings of the 2017 IEEE International Conference on Multimedia and Expo (ICME), Hong Kong, China, 10–14 July 2017; pp. 877–882.
38. Lim, B.; Son, S.; Kim, H.; Nah, S.; Lee, K.M., Enhanced Deep Residual Networks for Single Image Super-Resolution, In Proceedings of the 2017 IEEE Conference on Computer Vision and Pattern Recognition Workshops (CVPRW), Honolulu, HI, USA, 21–26 July 2017; pp. 1132–1140.
39. Haldar, J.P., Zhuo, J.: P-LORAKS: Low-rank modeling of local k-space neighborhoods with parallel imaging data. Magn. Reson. Med. 75(4), 1499–1514 (2016).

ICCS Camera Ready Version 2025
To cite this paper please use the final published version:
DOI: 10.1007/978-3-031-97554-7_25